analytical chemistry

pubs.acs.org/ac Article

Amplified Electrochemical Biosensing of Thrombin Activity by RAFT Polymerization

Qiong Hu, Yu Bao, Shiyu Gan, Yuwei Zhang,* Dongxue Han, and Li Niu

Cite This: https://dx.doi.org/10.1021/acs.analchem.9b05647 Read Online

ACCESS | Metrics & More | Article Recommendations | Supporting Information

ABSTRACT: As a serine protease, thrombin is a pivotal component in coagulation cascade and has been frequently screened as an informative biomarker for the diagnosis of coagulation disorder-related diseases. Herein, a "signal-on" electrochemical biosensor is described for the highly sensitive and selective detection of thrombin activity, by exploiting a thrombin-specific substrate peptide (Tb peptide) as the recognition element and reversible addition−fragmentation chain transfer (RAFT) polymerization for signal amplification. Specifically, the carboxyl-group-free Tb peptides are self-assembled onto gold electrode surface via the N-terminal cysteine residue and are used for the specific recognition of thrombin molecules. After the proteolytic cleavage of the Tb peptides, the carboxyl-group-containing RAFT agents (4-cyano-4-(phenylcarbonothioylthio)pentanoic acid, CPAD) are tethered to the free carboxyl termini of the truncated peptide fragments via the carboxylate-zirconium-carboxylate chemistry. The subsequent RAFT polymerization leads to the grafting of a polymer chain from each proteolytically cleaved site, enabling the recruitment of a large number of electroactive ferrocene (Fc) tags to the electrode surface when ferrocenylmethyl methacrylate (FcMMA) is used as the monomer. Under optimal conditions, the detection limit of the described thrombin biosensor is as low as 2.7 μU mL^{-1} (~0.062 pM), with a linear response over the range of 10−250 μU mL^{-1} (R^2 = 0.997). Results also indicate that the biosensor is highly selective and applicable to the detection of thrombin activity in complex serum samples and the screening of thrombin inhibitors. The described biosensor is low-cost and relatively easy in preparation and thus shows great promise for the highly sensitive and selective detection of thrombin activity.

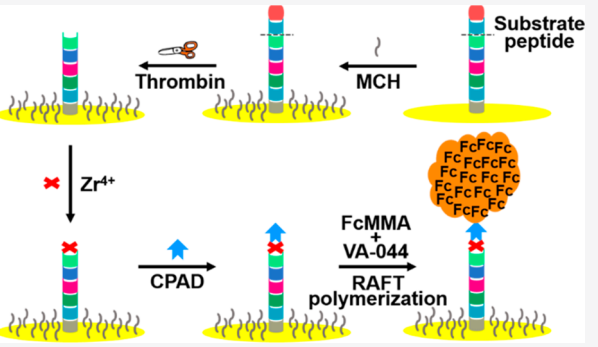

As a serine protease, thrombin (Tb) is the main effector protein of the coagulation cascade.[1] It acts directly on the last step of blood coagulation, by promoting the conversion of soluble fibrinogen in plasma into insoluble fibrin, the fibrous matrix of blood clots.[1] It also has a host of direct actions on various cellular processes, such as platelet activation and aggregation, endothelial activation, cytokine production, epithelial mitosis, and calcium signaling.[1] The abnormality of Tb expression has been found to be closely related to various human diseases such as thrombosis, myocardial infarction, atherosclerosis, hemophilia, inflammation, and tumor growth, metastasis, and angiogenesis.[1,2] Thus, the sensitive and selective detection of Tb activity is of significant importance to the evaluation of coagulation function and the diagnosis of coagulation disorder-related diseases.

The presence of Tb can be selectively detected by using such as the Tb-specific antibodies,[3,4] aptamers,[5−7] or substrate peptides[8,9] as the molecular recognition elements. The affinity assays based on the former two approaches are useful in the detection of Tb concentration,[10−12] and the proteolytic assays through the substrate peptide-based approach are applicable to the detection of Tb activity.[13] As the activity levels can reflect the true biological function of Tb, the substrate peptide-based approach is particularly useful in clinical applications. On the basis of the proteolytic cleavage of substrate peptides, various methods, such as colorimetric,[8] fluorescent,[14−16] bioluminescent,[17] surface-enhanced Raman scattering (SERS)-based,[18,19] photoelectrochemical (PEC),[20] and electrochemical,[21−25] have thus far been proposed for the detection of Tb activity. In view of the merits such as high sensitivity and selectivity, rapid response, low cost, and easy operation, electrochemical biosensors show great promise for the detection of Tb activity. For example, Adjémian et al.[21] and Ji et al.[22] described the use of the ferrocene- or *p*-aminodiphenylamine-labeled substrate peptide as the recognition element for the electrochemical biosensing of Tb activity, in which the proteolytic cleavage of substrate peptides led to the detachment of the electroactive tags from the electrode surface, and the decrease of detection signal corresponds to the increase of Tb activity. These two biosensors are low-cost and quite easy in preparation. Because

Received: December 15, 2019
Accepted: January 22, 2020

https://dx.doi.org/10.1021/acs.analchem.9b05647
Anal. Chem. XXXX, XXX, XXX−XXX

each substrate peptide was labeled with only an electroactive tag, however, their detection sensitivity is still not satisfactory. To improve the detection sensitivity, gold nanoparticles (AuNPs) and electrochemical-chemical-chemical redox cycling were, respectively, taken advantage of by Wang et al.[24] and Han et al.[25] to amplify the detection signal. Due to the involvement of tyrosinase and dopamine-modified AuNPs for signal amplification, the AuNPs-based strategy suffers from the drawbacks of high detection cost and complicated operation. Although easy to operate, the redox cycling-based strategy suffers from the drawback of low signal-to-background ratio. Besides, previous electrochemical biosensors are susceptible to the false-positive results, because a higher level of Tb activity eventually results in a lower detection signal (signal-off).

Discovered at the CSIRO of Australia in 1998,[26] reversible addition−fragmentation chain transfer (RAFT) polymerization is a powerful reversible deactivation radical polymerization (RDRP) method,[27] in which the RAFT process is mediated by a thiocarbonylthio compound (as the RAFT agent), such as dithiobenzoates, dithioesters, and trithiocarbonates.[28] RAFT polymerization is applicable to a wide range of vinyl monomers and tolerant to various functional groups and solvent systems, and through which complex polymers with well-defined architectures, low polydispersities, and predetermined molecular weights can be facilely synthesized.[29] In addition to its broad applications in the synthesis of polymers[30] and bioconjugates[31] and in the surface grafting,[32] RAFT polymerization has emerged as one of the most promising signal amplification strategies in the highly sensitive detection of clinically relevant biomolecules,[33] such as nucleic acids[34−36] and proteins.[37,38] Because it involves only the labeling of RAFT agents and the subsequent RAFT polymerization, the RAFT polymerization-based signal amplification strategy is highly efficient, low-cost, and easy to operate.[33]

In this work, we describe for the first time a "signal-on" electrochemical biosensor for the highly sensitive and selective detection of Tb activity, by using the Tb-specific substrate peptide (Tb peptide) as the molecular recognition element and the RAFT polymerization for signal amplification. The Tb peptide is free of carboxyl group and is immobilized through the N-terminus. The proteolytic cleavage of the Tb peptide can introduce a free carboxyl group at the C-terminus of the truncated fragment. As a result, the dithiobenzoate 4-cyano-4-(phenylcarbonothioylthio)pentanoic acid (CPAD) can be tethered to the electrode surface via carboxylate-zirconium-carboxylate chemistry.[35,37] With CPAD as the RAFT agent and ferrocenylmethyl methacrylate (FcMMA) as the monomer, the RAFT polymerization results in the grafting of a high density of long ferrocenyl polymer chains from the electrode surface, recruiting a large number of Fc tags for signal amplification. With the benefits from the proteolytic cleavage of substrate peptide and the RAFT polymerization-based signal amplification strategy, the described electrochemical biosensor can be applied to the highly sensitive and selective detection of Tb activity. Because a higher level of Tb activity can eventually result in a higher detection signal, in addition, it is a "signal-on" electrochemical biosensor, being tolerant to the false-positive results.[39] Its potential applications in the detection of Tb activity in complex serum samples and the screening of Tb inhibitors have also been demonstrated.

EXPERIMENTAL SECTION

Materials and Reagents. The carboxyl-group-free Tb peptide CGLVPRGS was custom-made by Ketai Biotechnology Co., Ltd. (Shanghai, China). Tb from bovine plasma (specific activity, ∼1176.5 U mg^{-1}; molecular weight, 37 KD) was purchased from Beijing Solarbio Science & Technology Co., Ltd. (Beijing, China). Hemoglobin (Hb), pepsin, alkaline phosphatase (ALP), CPAD, argatroban, zirconium dichloride oxide octahydrate ($ZrOCl_2$), 6-mercapto-1-hexanol (MCH), and FcMMA were provided by Sigma-Aldrich LLC. (St. Louis, MO). Lysozyme, normal human serum (NHS), γ-globulin, and lithium perchlorate trihydrate ($LiClO_4$) were obtained from Sangon Biotech (Shanghai) Co., Ltd. (Shanghai, China), YiJi Industrial Co., Ltd. (Shanghai, China), Yuanye Biotechnology Co., Ltd. (Shanghai, China), and Aladdin Bio-Chem Technology Co., Ltd. (Shanghai, China), respectively. Albumin from bovine serum (BSA), 2,2′-azobis[2-(2-imidazolin-2-yl)propane] dihydrochloride (VA-044), tris(hydroxymethyl)aminomethane (Tris), and 2-(*N*-morpholino)ethanesulfonic acid monohydrate (MES) were collected from J&K Scientific Ltd. (Shanghai, China). Anhydrous ethanol (EtOH) and other chemicals were supplied by Sinopharm Chemical Reagent Co., Ltd. (Shanghai, China). All chemicals (analytical grade or higher) were used as received. Ultrapure water (≥18.25 MΩ cm) was obtained from a Millipore Milli-Q water purification system.

Apparatus. Cyclic voltammetry (CV), linear sweep voltammetry (LSV), and square wave voltammetry (SWV) were performed with a CHI 760E electrochemical workstation (CH Instruments). Electrochemical impedance spectroscopy (EIS) was performed at the open circuit potential (0.18 V vs saturated calomel electrode (SCE)) with an Interface 1000 potentiostat (Gamry Instruments), in 0.1 M KNO_3 containing 5.0 mM $[Fe(CN)_6]^{3-/4-}$, with the frequency ranging from 100 kHz to 0.1 Hz and a potential amplitude of 5.0 mV. All electrochemical experiments were carried out at room temperature in a one-compartment cell with a conventional three-electrode system, consisting of a modified gold working electrode (ϕ = 3.0 mm), a platinum wire counter electrode, and a SCE reference electrode. A JEOL JSM-7100F field emission scanning electron microscope was used to collect the SEM image at an accelerating voltage of 15 kV.

Electrochemical Biosensing of Tb Activity. Prior to modification, the gold electrode surface was pretreated according to the following procedures.[35,37] First, it was hand-polished with 0.3 μm alumina slurry to a mirror-like finish and ultrasonically cleaned in EtOH and ultrapure water. After a treatment with fresh piranha solution (a 3:1 (v/v) mixture of H_2SO_4 (98%) and H_2O_2 (30%); *Caution: This solution is strongly oxidative and must be handled with extreme care*), the electrode surface was ultrasonically cleaned in ultrapure water. After that, it was treated in 0.5 M H_2SO_4 solution with CV by cycling the potential at a scan rate of 0.1 V s^{-1} between −0.3 and 1.5 V until a stable curve was observed. After a rigorous ultrasonic cleaning with ultrapure water and drying with N_2, the resulting electrode surface was ready for modification.

Subsequently, 10 μL of 1.5 μM Tb peptide aqueous solution was added to the electrode surface, followed by an incubation at 37 °C for 60 min and a rigorous rinsing with ultrapure water. After the blocking with 2.0 mM MCH solution (60% EtOH) at 37 °C for 15 min, the electrode surface was sequentially rinsed with EtOH and ultrapure water. Then 15 μL of Tb solution

https://dx.doi.org/10.1021/acs.analchem.9b05647
Anal. Chem. XXXX, XXX, XXX−XXX

(20 mM Tris-HCl, 150 mM NaCl, pH 8.0) was added to the electrode surface, followed by an incubation at 37 °C for 60 min. After a rigorous rinsing with ultrapure water (to avoid the physical adsorption of Tb molecules), the electrode surface was immersed in 5.0 mM $ZrOCl_2$ solution (20% EtOH). After an incubation at 37 °C for 30 min, the resulting surface was rinsed with ultrapure water. Afterward, it was immersed in 0.5 mM CPAD solution (20% EtOH), incubated at 37 °C for 30 min, and rigorously rinsed with EtOH and ultrapure water. Following this, the electrode surface was immersed in the RAFT polymerization solution (a fresh EtOH aqueous solution of FcMMA and VA-044; the concentration of FcMMA was 0.15 mM, and the concentrations of VA-044 and EtOH were optimized), followed by an incubation at 47 °C for 1.5 h. Lastly, the as-modified electrode surface was rigorously rinsed with EtOH and ultrapure water, dried with N_2, and measured in 0.5 M $LiClO_4$ solution with SWV, with a quiet time of 15 s, an increase potential of 4.0 mV, and a potential amplitude of 25 mV.

RESULTS AND DISCUSSION

Principle of the Electrochemical Biosensing of Tb Activity. The principle of the described electrochemical Tb biosensor is illustrated in Scheme 1. For the highly selective detection of Tb activity, the Tb peptides are used herein as the molecular recognition elements and are tethered to the gold electrode surface via the N-terminal cysteine residue. The hexapeptide fragment LVPRGS located at the C-terminus of the Tb peptide has been verified to be an ideal substrate for Tb,[18] and the proteolytic cleavage site is immediately behind the arginine (Arg) residue, i.e., the Arg-Gly bond.[9] In the Tb peptide, the free carboxyl group on the serine (Ser) residue has been blocked by amination. However, the proteolytic cleavage of the Tb peptides can produce the free carboxyl-group termini. Thus, only after the proteolytic cleavage of the Tb peptides can the RAFT agents CPAD be tethered to the electrode surface via the Zr(IV) linkers. Such a design can thus avoid the possible false-positive results caused by the nonspecific adsorption. For the highly sensitive detection of Tb activity, on the other hand, RAFT polymerization is exploited for signal amplification. With CPAD as the RAFT agent and FcMMA as the monomer, in this work, RAFT polymerization is initiated via thermal decomposition of the water-soluble initiators, VA-044.[33,35] Through the RAFT polymerization, a large number of Fc tags can be recruited to the electrode surface for a significant amplification of the detection signal.[33] As a result, the combined use of substrate peptide as the recognition element and RAFT polymerization for signal amplification allows the highly sensitive and selective detection of Tb activity. In addition, because the detection signal increases with the increase of Tb activity, the described electrochemical Tb biosensor is tolerant to the false-positive results.

Scheme 1. "Signal-on" Electrochemical Biosensing of Tb Activity

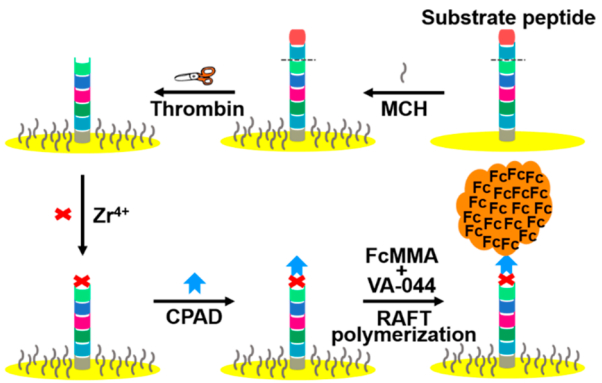

Characterizations. The surface coverage (Γ_m) of Tb peptide on the gold electrode is determined to be 3.15×10^{-10} mol cm^{-2}, through the reductive desorption of thiol based on LSV (Figure S1).[40] Further, the feasibility of the electrochemical biosensing of Tb activity was studied based on a series of control experiments. The SWV curves of the differently modified electrodes are shown in Figure 1A. For the as-modified electrode, a strong oxidation current can be clearly observed. The oxidation current can be assigned to the electrochemical oxidation of the Fc tags.[41] The resulting peak potential is located at ~0.27 V vs SCE, and the value falls within the typical oxidation potential range of Fc in $LiClO_4$ aqueous solutions.[39,42] For the electrodes modified without Tb peptides, Tb enzymes, Zr(IV) linkers, RAFT agents (CPAD), VA-044 initiators, or FcMMA monomers, on the other hand, almost no oxidation current can be observed. These results confirm that it is feasible to detect the activity of Tb based on the described biosensor. The very low background signal can be ascribed to the elaborately designed protocol, which can effectively avoid the nonspecific adsorption. As an example, without the proteolytic cleavage of the Tb peptides, no functional sites are available on the electrode surface for the tethering of the RAFT agents CPAD via the Zr(IV) linkers. Besides, such a high signal-to-background ratio makes the highly sensitive detection of Tb activity possible.

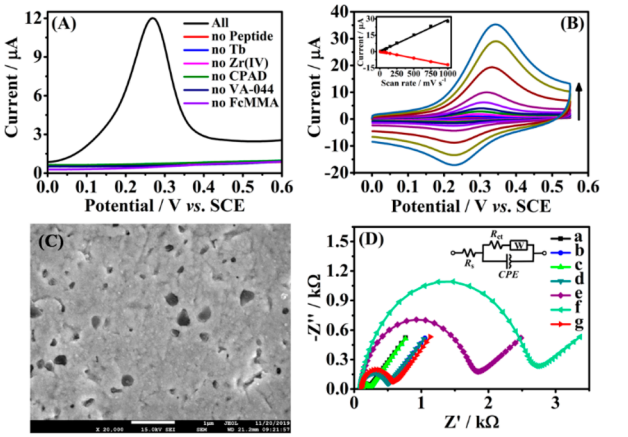

Figure 1. (A) SWV curves of the as-modified electrode and of those modified without Tb peptides, Tb enzymes, Zr(IV) linkers, RAFT agents, VA-044 initiators, or FcMMA monomers. (B) CV curves of the as-modified electrode in 0.5 M $LiClO_4$ at various scan rates. Inset shows the plots of the redox peak currents versus the scan rate. (C) SEM image of the as-modified electrode. (D) Nyquist plots of the bare gold electrode (a) and of those obtained after the modification of Tb peptides (b) and MCH (c), the proteolytic cleavage of the Tb peptides by Tb enzymes (d), the modification of Zr(IV) linkers (e), RAFT agents (f), and ferrocenyl polymers (g). Inset depicts the equivalent circuit (R_s, solution resistance; W, Warburg resistance; CPE, constant-phase element). Tb, 250 μU mL^{-1}; EtOH, 60%; VA-044, 150 μM.

https://dx.doi.org/10.1021/acs.analchem.9b05647
Anal. Chem. XXXX, XXX, XXX−XXX

The redox properties of the Fc/Fc^+ couple were investigated by CV. As can be seen from Figure 1B, the redox peak currents of the cyclic voltammograms are increased linearly with the increase of scan rate, and this is in line with the fact that the Fc tags are tethered to the electrode surface.[39,42] In addition, the less ideal reversibility of the redox waveforms can be ascribed to the complicated monolayers, which interfere with the interfacial charge transfer.[41] As the scan rate increases, the redox peak potentials shift, because the interfacial charge transfer becomes slower than the scan rate.[43]

After the RAFT polymerization, the surface morphology of the modified electrode was probed by SEM. As shown in Figure 1C, a densely packed polymer layer is present on the electrode surface,[38,41] indicating that RAFT polymerization is highly efficient as a signal amplification strategy.[35] The elemental mapping of the polymer layer was interrogated by energy-dispersive X-ray spectroscopy. The traces of Fe element, as shown in Figure S2, verify the presence of the ferrocenyl polymers.[35−38]

The stepwise modification of the electrode surface was characterized by EIS. The typical Nyquist plots of the impedance spectra are shown in Figure 1D. As expected, the bare gold electrodes exhibit a small charge-transfer resistance (R_{ct}) (~126 Ω, plot a), indicating the fast charge transfer kinetics. The assembly of the Tb peptides leads to an increase of the R_{ct} (~401 Ω, plot b), and this can be ascribed to the steric hindrance from the peptidyl monolayer.[37,42] The MCH blocking of the remaining binding sites results in a significant decrease of the R_{ct} (~113 Ω, plot c), and the value is even much lower than that of the electrodes modified with only an MCH layer (results not shown). Identical results have been observed from the repeated experiments and without exception, which indicates that the backfilling of the Tb peptide monolayer with MCH molecules can greatly facilitate the interfacial charge transfer. The underlying mechanism is unclear, presumably due to the fact that the Tb peptide molecules alone are in a lying-down configuration due to the presence of nonspecific interactions with the electrode surface and they are forced to rearrange into a standing-up configuration by the MCH layer, thereby decreasing the steric hindrance.[44] The proteolytic cleavage of the Tb peptides is accompanied by an increase of the R_{ct} to ~384 Ω (plot d), because the negatively charged carboxyl group termini are repulsive to the $[Fe(CN)_6]^{3-/4-}$ probes.[37,41] The chelation of the Zr(IV) linkers (~1.67 kΩ, plot e) and the tethering of the RAFT agents (~2.52 kΩ, plot f) result in the increases of the R_{ct}, which are in line with the previous reports.[35−38] After the RAFT polymerization, the R_{ct} decreases to ~473 Ω (plot g). Owing to a significant increase of the steric hindrance, the presence of a polymer layer on the electrode surface is adverse to the interfacial charge transfer. However, the ferrocenyl polymers are electroactive, which can on the other hand facilitate the interfacial charge transfer. As a matter of fact, we have found that the grafting of more electroactive ferrocenyl polymers on the electrode surface can result in a smaller R_{ct}.[35] Therefore, the significant decrease of the R_{ct} caused by the RAFT polymerization indicates the presence of a densely packed ferrocenyl polymer layer on the electrode surface, which is in good agreement with the observation of SEM characterization. These results demonstrate that the electrode surface has been successfully modified as expected.

Effects of Experimental Conditions. In the RAFT polymerization, the radical initiator (VA-044) is water-soluble, whereas the FcMMA monomer and the ferrocenyl polymer are not. As a result, here should be a trade-off between the solubility of these components. In this work, the EtOH aqueous solution was used as the solvent system. For a high polymerization efficiency, the effect of EtOH concentration on the RAFT polymerization was investigated. As can be seen from Figure S3A, the peak current increases with the increase of the concentration of EtOH in the RAFT polymerization solution from 10% to 60%, and then it decreases with the further increase of EtOH concentration. Thus, the 60% EtOH aqueous solution is optimal as the solvent system for the RAFT polymerization.

Due to the irreversible radical−radical termination, the RAFT polymerization requires a continuous supply of the initiating radicals.[33] In this work, the RAFT polymerization was performed without deoxygenating. More initiating radicals are thus required for the consumption of the dissolved oxygen, because the propagating radicals are sensitive to it.[33] Besides, a higher concentration of initiating radicals is essential for a higher polymerization rate. However, the initiating radicals can also terminate the RAFT polymerization by reacting with the propagating radicals. Thus, the concentration of the radical initiator VA-044 should be optimized. As can be seen from Figure S3B, the peak current increases with the increase of VA-044 concentration from 30 μM to 150 μM, and then it decreases with the further increase of VA-044 concentration. Therefore, the optimal concentration of VA-044 is 150 μM.

Analytical Performance. Under optimal conditions, the described electrochemical biosensor was challenged with the quantitative analysis of Tb activity. Figure 2A shows the

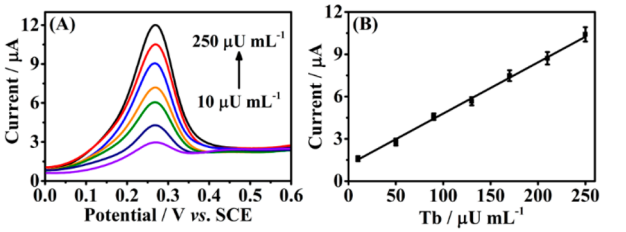

Figure 2. (A) SWV curves toward various Tb activities (10−250 μU mL^{-1}). (B) Calibration plot of peak current versus Tb activity.

activity-dependent SWV curves. As can be seen, the peak current of the SWV curve increases with the increase of Tb activity from 10 μU mL^{-1} to 250 μU mL^{-1}. This is to be expected, because a higher Tb activity can eventually result in the recruitment of more Fc tags. The described electrochemical Tb biosensor is tolerant to the false-positive results, due to the "signal-on" mode. The plot of peak current with Tb activity is shown in Figure 2B. As can be seen, the peak current is linearly related to Tb activity over the range of 10−250 μU mL^{-1} (R^2 = 0.997). The regression equation is $y = 0.036x + 1.16$ (where y is the peak current in μA, and x is the activity of Tb in μU mL^{-1}), and the limit of detection (LOD) is 2.7 μU mL^{-1} (~0.062 pM), according to the $3\sigma_b$/slope criteria (σ_b, the standard deviation of the blank control). As shown in Table S1, the LOD is much lower than that of most of the previous methods described for the detection of Tb activity. Such a high sensitivity, to a large extent, can be ascribed to the RAFT polymerization-based signal amplification strategy, through which numerous Fc tags can be recruited to the electrode surface. Tb is almost absent in the blood of healthy

https://dx.doi.org/10.1021/acs.analchem.9b05647
Anal. Chem. XXXX, XXX, XXX−XXX

subjects.[45] In the blood of patients suffering from the coagulation disorder-related diseases, it can only reach high picomolar levels.[46] Thus, the described electrochemical Tb biosensor shows great promise for clinical and diagnostic applications.

The intra- and intercoefficients of variation of the five replicate assays of Tb activity with the identically modified electrodes at 250 μU mL^{-1} are 4.8% and 5.3%, respectively, indicating a good reproducibility of the electrochemical biosensing of Tb activity. In addition, the as-modified electrodes (Tb, 250 μU mL^{-1}) show satisfactory storage stability, because even after a storage at 4 °C for 2 weeks, no significant decrease of the peak current can be observed.

Selectivity and Practicability. The selectivity was confirmed using several nontarget proteins, such as ALP, BSA, globulin, Hb, pepsin, and lysozyme. The concentrations of these interferents were 10-fold of that of the Tb enzyme. Figure 3 shows the peak currents in the presence of Tb enzyme

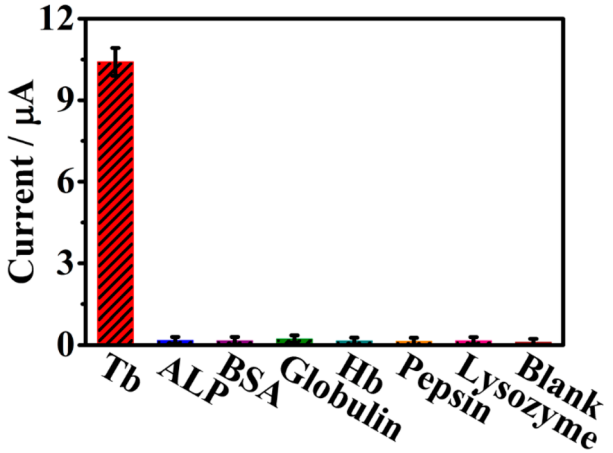

Figure 3. Peak currents toward different enzymes/proteins. Tb, 250 μU mL^{-1} (~0.21 ng mL^{-1}); others, 2.1 ng mL^{-1}.

or the interferents. For the Tb enzyme at 250 μU mL^{-1} (~0.21 ng mL^{-1}), a strong peak current can be observed. To the contrary, the interferents at a concentration of as high as 2.1 ng mL^{-1} cannot result in significant change on the peak current relative to that of the blank control. These results essentially indicate that this biosensor is highly selective, which can be ascribed to the excellent specificity of an enzyme (Tb enzyme) toward its substrate (Tb peptide).

The detection of Tb activity in real biological samples is clinically relevant. The practicability of the described electrochemical Tb biosensor was investigated in the presence of normal human serum (NHS) as the complex biological matrix. Although it is composed of a large number of biomolecules, NHS does not contain any coagulation factors such as Tb.[45] The three spiked serum samples (50 μU mL^{-1}, 150 μU mL^{-1}, and 250 μU mL^{-1}) were prepared with 10% NHS. The results of the standard addition experiments are shown in Table 1.

Table 1. Detection of Tb Activity in Spiked Serum Samples

sample	added (μU mL^{-1})	found (μU mL^{-1})	recovery (%)	RSD (%, n = 5)
1	50	52.1	104.2	5.3
2	150	151.8	101.2	5.1
3	250	242.1	~96.8	4.8

The recoveries are from 96.8% to 104.2% with the relative standard deviation (RSD) around 5.0%, indicating that the described biosensor has the potential to be applied to the detection of Tb activity in complex serum samples.

Inhibitor Screening. The overexpression of Tb has been found to be implicated in thrombosis and other coagulation disorder-related diseases.[47] Tb inhibitors are useful as anticoagulants such as in molecular targeted therapy, hemostasis, and fundamental biochemical research. The potential application of the described biosensor in inhibitor screening was studied using argatroban (a direct, selective Tb inhibitor[48]) as the model. As shown in Figure 4A, the peak

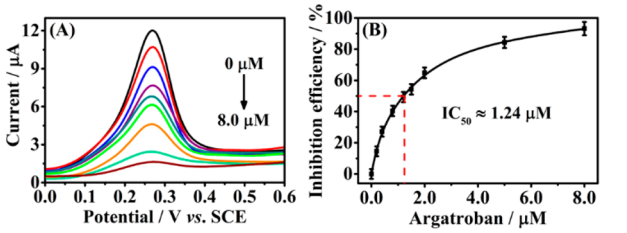

Figure 4. (A) SWV curves toward various concentrations of argatroban (0–8.0 μM). (B) Dependence of inhibition efficiency on argatroban concentration. Tb, 250 μU mL^{-1}.

current decreases with the increase of argatroban concentration, indicating that argatroban as an inhibitor can effectively lower the cleavage efficiency of the Tb peptides. The dose-dependent inhibition efficiency plot is shown in Figure 4B. The half-maximal inhibitory concentration (IC_{50}) for argatroban is estimated to be 1.24 μM, which is close to the reported value.[20] Thus, this biosensor is applicable to inhibitor screening.

CONCLUSIONS

In summary, a "signal-on" biosensor has been described for the electrochemical detection of Tb activity, by using the Tb-specific substrate peptide as the molecular recognition element and RAFT polymerization for signal amplification. Substrate peptides are low-priced and easy to synthesize and modify, as well as show high chemical/thermal stability. The biosensor is applicable to the direct detection of Tb activity, which can reflect the true biological function of the Tb enzyme. The RAFT polymerization-based signal amplification strategy is highly efficient, low-cost, and easy to operate, through which a high detection signal is obtainable even in the presence of a low level of Tb activity, thereby greatly improving the detection sensitivity. The described electrochemical Tb biosensor is highly selective and the LOD can be as low as 2.7 μU mL^{-1} (~0.062 pM). Moreover, it is applicable to the detection of Tb activity in complex serum samples as well as the screening of Tb inhibitors. Because it is low-cost, relatively easy in preparation, and tolerant to the false-positive results, the described biosensor shows great promise for the highly sensitive and selective detection of Tb activity.

ASSOCIATED CONTENT

Supporting Information

The Supporting Information is available free of charge at https://pubs.acs.org/doi/10.1021/acs.analchem.9b05647.

Figures including (1) reductive desorption of Tb peptides using LSV, (2) elemental mapping of the as-

https://dx.doi.org/10.1021/acs.analchem.9b05647
Anal. Chem. XXXX, XXX, XXX−XXX

modified electrode, and (3) effects of experimental conditions. Table of analytical performance of different methods for Tb activity detection (PDF)

AUTHOR INFORMATION

Corresponding Author

Yuwei Zhang − *Center for Advanced Analytical Science, School of Chemistry and Chemical Engineering, Guangzhou University, Guangzhou 510006, P. R. China;* orcid.org/0000-0002-3040-137X; Phone: +86-020-39366902; Email: ccywzhang@gzhu.edu.cn

Authors

Qiong Hu − *Center for Advanced Analytical Science, School of Chemistry and Chemical Engineering and School of Civil Engineering, Guangzhou University, Guangzhou 510006, P. R. China;* orcid.org/0000-0001-6360-1813

Yu Bao − *Center for Advanced Analytical Science, School of Chemistry and Chemical Engineering, Guangzhou University, Guangzhou 510006, P. R. China;* orcid.org/0000-0002-5023-4345

Shiyu Gan − *Center for Advanced Analytical Science, School of Chemistry and Chemical Engineering, Guangzhou University, Guangzhou 510006, P. R. China;* orcid.org/0000-0002-5495-4585

Dongxue Han − *Center for Advanced Analytical Science, School of Chemistry and Chemical Engineering and School of Civil Engineering, Guangzhou University, Guangzhou 510006, P. R. China;* orcid.org/0000-0002-7343-2221

Li Niu − *Center for Advanced Analytical Science, School of Chemistry and Chemical Engineering and School of Civil Engineering, Guangzhou University, Guangzhou 510006, P. R. China; Collaborative Innovation Center of Tumor Marker Detection Technology, Equipment and Diagnosis-Therapy Integration in Universities of Shandong, Shandong Province Key Laboratory of Detection Technology for Tumor Makers, School of Chemistry and Chemical Engineering, Linyi University, Linyi 276005, P. R. China;* orcid.org/0000-0003-3652-2903

Complete contact information is available at: https://pubs.acs.org/10.1021/acs.analchem.9b05647

Author Contributions

All authors have given approval to the final version of the manuscript.

Notes

The authors declare no competing financial interest.

ACKNOWLEDGMENTS

This work was supported by the National Natural Science Foundation of China (21904026), the Project Funded by China Postdoctoral Science Foundation (2018M643040), and the National Natural Science Foundation of China (21974031, 21974032, and 21974033).

REFERENCES

(1) Coughlin, S. R. *Nature* **2000**, *407*, 258−264.
(2) Nierodzik, M. L.; Karpatkin, S. *Cancer Cell* **2006**, *10*, 355−362.
(3) He, P.; Shen, L.; Cao, Y.; Li, D. *Anal. Chem.* **2007**, *79*, 8024−8029.
(4) Kang, Y.; Feng, K. J.; Chen, J. W.; Jiang, J. H.; Shen, G. L.; Yu, R. Q. *Bioelectrochemistry* **2008**, *73*, 76−81.
(5) Choi, J. H.; Chen, K. H.; Strano, M. S. *J. Am. Chem. Soc.* **2006**, *128*, 15584−15585.
(6) Xiao, Y.; Lubin, A. A.; Heeger, A. J.; Plaxco, K. W. *Angew. Chem., Int. Ed.* **2005**, *44*, 5456−5459.
(7) Chang, H.; Tang, L.; Wang, Y.; Jiang, J.; Li, J. *Anal. Chem.* **2010**, *82*, 2341−2346.
(8) Guarise, C.; Pasquato, L.; De Filippis, V.; Scrimin, P. *Proc. Natl. Acad. Sci. U. S. A.* **2006**, *103*, 3978−3982.
(9) Pinto, M. R.; Schanze, K. S. *Proc. Natl. Acad. Sci. U. S. A.* **2004**, *101*, 7505−7510.
(10) Shangguan, L.; Zhu, W.; Xue, Y.; Liu, S. *Biosens. Bioelectron.* **2015**, *64*, 611−617.
(11) Shen, G.; Zhang, H.; Yang, C.; Yang, Q.; Tang, Y. *Anal. Chem.* **2017**, *89*, 548−551.
(12) Yang, J.; Dou, B.; Yuan, R.; Xiang, Y. *Anal. Chem.* **2017**, *89*, 5138−5143.
(13) Medintz, I. L.; Clapp, A. R.; Brunel, F. M.; Tiefenbrunn, T.; Uyeda, H. T.; Chang, E. L.; Deschamps, J. R.; Dawson, P. E.; Mattoussi, H. *Nat. Mater.* **2006**, *5*, 581−589.
(14) Wu, M.; Petryayeva, E.; Algar, W. R. *Anal. Chem.* **2014**, *86*, 11181−11188.
(15) Li, L.; Lin, H.; Lei, C.; Nie, Z.; Huang, Y.; Yao, S. *Biosens. Bioelectron.* **2014**, *54*, 42−47.
(16) Zhang, M.; Yin, B. C.; Wang, X. F.; Ye, B. C. *Chem. Commun.* **2011**, *47*, 2399−2401.
(17) Chen, L.; Bao, Y.; Denstedt, J.; Zhang, J. *Biosens. Bioelectron.* **2016**, *77*, 83−89.
(18) Wu, Z.; Liu, Y.; Liu, Y.; Xiao, H.; Shen, A.; Zhou, X.; Hu, J. *Biosens. Bioelectron.* **2015**, *65*, 375−381.
(19) Wu, Z.; Liu, Y.; Zhou, X.; Shen, A.; Hu, J. *Biosens. Bioelectron.* **2013**, *44*, 10−15.
(20) Wang, J.; Song, M.; Hu, C.; Wu, K. *Anal. Chem.* **2018**, *90*, 9366−9373.
(21) Adjémian, J.; Anne, A.; Cauet, G.; Demaille, C. *Langmuir* **2010**, *26*, 10347−10356.
(22) Ji, J.; Gan, J.; Kong, J.; Yang, P.; Liu, B.; Ji, C. *Electrochem. Commun.* **2012**, *16*, 53−56.
(23) Cahill, K.; Suttmiller, R.; Oehrle, M.; Sabelhaus, A.; Gemene, K. L. *Electroanalysis* **2017**, *29*, 448−455.
(24) Wang, X.; Wang, G.; Li, C.; Wang, J.; Xia, N. *Int. J. Electrochem. Sci.* **2013**, *8*, 8210−8217.
(25) Han, G. C.; Hou, J. T.; Feng, X. Z.; Huang, Z. L.; Gu, W.; Chen, Z. C. *Int. J. Electrochem. Sci.* **2016**, *11*, 8646−8653.
(26) Chiefari, J.; Chong, Y. K.; Ercole, F.; Krstina, J.; Jeffery, J.; Le, T. P. T.; Mayadunne, R. T. A.; Meijs, G. F.; Moad, C. L.; Moad, G.; Rizzardo, E.; Thang, S. H. *Macromolecules* **1998**, *31*, 5559−5562.
(27) Perrier, S. *Macromolecules* **2017**, *50*, 7433−7447.
(28) Keddie, D. J.; Moad, G.; Rizzardo, E.; Thang, S. H. *Macromolecules* **2012**, *45*, 5321−5342.
(29) Hill, M. R.; Carmean, R. N.; Sumerlin, B. S. *Macromolecules* **2015**, *48*, 5459−5469.
(30) Keddie, D. J. *Chem. Soc. Rev.* **2014**, *43*, 496−505.
(31) Boyer, C.; Bulmus, V.; Davis, T. P.; Ladmiral, V.; Liu, J.; Perrier, S. *Chem. Rev.* **2009**, *109*, 5402−5436.
(32) Gonzato, C.; Courty, M.; Pasetto, P.; Haupt, K. *Adv. Funct. Mater.* **2011**, *21*, 3947−3953.
(33) Hu, Q.; Gan, S.; Bao, Y.; Zhang, Y.; Han, D.; Niu, L. Controlled/"living" radical polymerization-based signal amplification strategies for biosensing. *J. Mater. Chem. B* **2020**, DOI: 10.1039/C9TB02419K.
(34) He, P.; Zheng, W.; Tucker, E. Z.; Gorman, C. B.; He, L. *Anal. Chem.* **2008**, *80*, 3633−3639.
(35) Hu, Q.; Han, D.; Gan, S.; Bao, Y.; Niu, L. *Anal. Chem.* **2018**, *90*, 12207−12213.
(36) Hu, Q.; Kong, J.; Han, D.; Niu, L.; Zhang, X. *ACS Sens.* **2019**, *4*, 235−241.
(37) Hu, Q.; Kong, J.; Han, D.; Zhang, Y.; Bao, Y.; Zhang, X.; Niu, L. *Anal. Chem.* **2019**, *91*, 1936−1943.
(38) Hu, Q.; Kong, J.; Han, D.; Bao, Y.; Zhang, X.; Zhang, Y.; Niu, L. *Talanta* **2020**, *206*, 120173.

(39) Fan, C.; Plaxco, K. W.; Heeger, A. J. *Proc. Natl. Acad. Sci. U. S. A.* **2003**, *100*, 9134−9137.
(40) Chi, Q.; Zhang, J.; Ulstrup, J. *J. Phys. Chem. B* **2006**, *110*, 1102−1106.
(41) Hu, Q.; Wang, Q.; Sun, G.; Kong, J.; Zhang, X. *Anal. Chem.* **2017**, *89*, 9253−9259.
(42) Hu, Q.; Wang, Q.; Jiang, C.; Zhang, J.; Kong, J.; Zhang, X. *Biosens. Bioelectron.* **2018**, *110*, 52−57.
(43) Paul, A.; Bezer, S.; Venkatramani, R.; Kocsis, L.; Wierzbinski, E.; Balaeff, A.; Keinan, S.; Beratan, D. N.; Achim, C.; Waldeck, D. H. *J. Am. Chem. Soc.* **2009**, *131*, 6498−6507.
(44) Revenga-Parra, M.; García, T.; Pariente, F.; Lorenzo, E.; Alonso, C. *Electroanalysis* **2011**, *23*, 100−107.
(45) Bini, A.; Minunni, M.; Tombelli, S.; Centi, S.; Mascini, M. *Anal. Chem.* **2007**, *79*, 3016−3019.
(46) Bichler, J.; Heit, J. A.; Owen, W. G. *Thromb. Res.* **1996**, *84*, 289−294.
(47) Sambrano, G. R.; Weiss, E. J.; Zheng, Y. W.; Huang, W.; Coughlin, S. R. *Nature* **2001**, *413*, 74−78.
(48) Walenga, J. M. *Pathophysiol. Haemostasis Thromb.* **2002**, *32*, 9−14.

https://dx.doi.org/10.1021/acs.analchem.9b05647
Anal. Chem. XXXX, XXX, XXX−XXX